Surface-enhanced second-harmonic generation in nonlinear corrugated dielectrics: new theoretical approaches

E. Popov* and M. Nevière

Laboratoire d'Optique Electromagnétique, Case 262, Faculté des Sciences et Techniques de Saint Jérôme, Avenue Escadrille Normandie-Niemen, 13397 Marseille, Cedex 20, France

Received November 24, 1993; revised manuscript received April 22, 1994

A new rigorous electromagnetic theory is developed for studying the second-harmonic generation process that occurs when a high-power laser beam falls on a periodically corrugated waveguide. The waveguide can consist of several layers with corrugated or plane boundaries, with at least one of the layers being filled with a nonlinear lossless or lossy dielectric. The theory uses a nonorthogonal coordinate transformation, which maps the corrugated interfaces onto planes. The Maxwell equations written in covariant form lead to a set of first-order partial differential equations with nonconstant coefficients. Taking into account the periodicity of the system, this set of equations could be transformed into a set of ordinary differential equations with constant coefficients, which can be resolved by an eigenvalue–eigenvector technique, avoiding numerical integration. The theory is developed for both TE and TM polarizations and for any groove geometry and incidence; it can be used, in particular, when surface waves (guided modes or surface plasmon–polaritons) are excited. It is a powerful tool for studying the enhancement of the second-harmonic generation resulting from local field enhancement by electromagnetic resonances. In addition an approach based on the Rayleigh hypothesis is developed. Both theoretical approaches are compared with previously developed differential theory for gratings in nonlinear optics. A spectacular agreement is obtained between the three theories for both TE and TM polarization. The new method is free of limitations concerning the waveguide thickness, the groove depth, and the conductivity of the grating material. It is demonstrated that the limitations of the Rayleigh hypothesis are stronger at the second-harmonic frequency.

1. INTRODUCTION

Second-harmonic generation by metals and dielectrics has attracted a great deal of interest from both theoretical and experimental viewpoints.[1–9] The great sensitivity of this phenomenon to submicroroughness makes it a competitive candidate for nondestructive surface characterization, whereas the discovery of new organic components with high second-order nonlinear susceptibilities opens the possibility of making frequency doublers of high performance. The small thicknesses of optical waveguides lead to high power densities, which are required for observing a significant second-harmonic signal. Such power densities can be further increased by several orders of magnitude if a surface wave is excited in the nonlinear medium. It may be a guided mode, existing for both TE or TM polarization, or a surface plasmon–polariton that occurs for metallic substrates in the visible and the near-infrared regions. The resonance excitation results in a strong enhancement of the local field and thus of the second-order nonlinear polarization, which acts as a source for the signal at the doubled frequency.

This process can be achieved in a prism coupler configuration, but in a planar geometry a grating coupler (namely, a corrugated waveguide) must be used. The planarity is not the only or the main consideration: the grating permits phase matching to a resonance at the second-harmonic frequency, which otherwise could hardly be achieved owing to the dispersion of the medium and the waveguide properties. We are then confronted with the problem of second-harmonic generation in a grating or, specifically, in a stack of layers with modulated and flat interfaces. The diffraction of light in nonlinear optics was previously studied with both the classical differential[9,10] and integral[11] formalisms for dielectric[9] and metallic[10,11] surfaces. Metallic interfaces give rise to the problem of writing the boundary conditions at the signal frequency,[1] which was solved in Ref. 12. Dielectric gratings lead to simpler analyses to the degree that the usual undepleted-pump approximation[13] can be assumed. The idea of this approximation is that the electric field of the incident and the diffracted waves at the initial frequency ω inside the nonlinear medium acts as a source for field generation at 2ω, and it is assumed that the second-harmonic generation is so weak (it really is) that its influence on the field at the initial frequency is negligible. This hypothesis is valid in the predominant number of cases, the only exception, to our knowledge, being the radiation of a waveguide mode propagating in a nonlinear corrugated waveguide when the radiation is carried through diffraction orders only at the second-harmonic frequency. Excluding the latter case, the undepleted-pump approximation allows a decoupling of the Maxwell equations at the two circular frequencies ω and 2ω. It is then possible to define a three-step analysis[9]: first, the electromagnetic field at the pump frequency is determined everywhere and, in particular, inside the nonlinear medium by a rigorous method for light diffraction by the corrugated system; second, these results are used to determine the nonlinear polarization at the second-harmonic frequency; and, third, the signal generated by this source term at 2ω is calculated, again

0740-3224/94/091555-10$06.00

by a rigorous method. Such a scheme was recently extended to a guiding geometry.[13] The integral method, at least at the present state of the art, is not suitable for dealing with dielectrics in nonlinear optics, because there are volume source terms to be taken into account. This is why the theory developed in Ref. 13 uses the differential method. It is well suitable for TE polarization but presents serious limitations concerning the groove depths of metallic gratings used in TM polarization. On top of that, if the thickness of the waveguide is large enough, numerical instabilities are noticed because of the loss of precision caused by the exponentially growing terms.

Our aim here is to present a new theoretical approach that does not suffer from these disadvantages. We are staying within the undepleted-pump-approximation scheme, and we use a rigorous method for analyzing light diffraction by corrugated surfaces and a stack of layers. The initial starting point is the work of Chandezon *et al.*,[14,15] further developed for cases in which only one of the interfaces is corrugated.[16] The choice of method was determined by its validity for deep and very deep gratings with lossless or lossy dielectric media or highly conducting materials, independent of the incident-wave polarization.[17,18] The only noticed limitation of the method concerns its inability to deal with profiles with very steep slopes (namely, lamellar and quasi-lamellar gratings).

Section 2 gives a detailed description of the formalism. We have to repeat some details from papers that have already been published, but this is necessary to introduce the notation that is used below in determining the nonlinear source term and to show how we are solving the problem with growing exponential functions. In Section 3 we give explicitly the formulas obtained when the Rayleigh hypothesis is applied to the problem under investigation. The parallelism of the two formalisms was previously pointed out,[17] but the main difference again has to be emphasized: whereas the first method is rigorous, methods based on the Rayleigh hypothesis are, in general, approximate. The validity of the latter methods has been extensively discussed,[19] and they give good results for sinusoidal gratings but usually fail for other profiles unless the groove depth is quite small. Nevertheless, it appears useful to have a code based on the Rayleigh hypothesis, because it is quite simple to implement in a computer and can be used for testing the results during the preparation of the code based on the rigorous method. A comparison between the results of the rigorous theory, presented in Section 2, with the results of the Rayleigh method and of the method based on the classical differential formalism is given in Section 4. The agreement between the results of the three theories is very good both for TE and TM polarization and for metallic or dielectric substrates. Whereas the Rayleigh method gives reliable results even for deep gratings (modulation depth exceeding 40%) at the initial frequency (linear response), at the nonlinear frequency it can diverge.

2. RIGOROUS THEORETICAL METHOD

A plane wave with wavelength λ is incident upon a multilayered periodically corrugated system (Fig. 1). Some of the notation used below is introduced in this figure. The plane of incidence is perpendicular to the grooves. For simplicity it is assumed in what follows that the system consists of two interfaces, one of them flat and the other corrugated. All the media are lossless or lossy dielectrics, and the intermediate layer has nonlinear properties that lead to second-harmonic generation.

In a general covariant form Maxwell's equations could be written as

$$\text{curl } \mathbf{E} = -\frac{\partial \mathbf{B}}{\partial t}, \qquad \text{curl } \mathbf{H} = \frac{\partial \mathbf{D}}{\partial t}, \tag{1}$$

where $\mathbf{E}$ and $\mathbf{H}$ denote electric- and magnetic-field vectors. In the undepleted-pump approximation the field at a circular frequency ω does not depend on the field at 2ω. Then Eqs. (1) have different forms at the two frequencies: at $\tilde{\omega}$,

$$\text{curl } \mathcal{E} = i\tilde{\omega}\tilde{\mu}\mathcal{H}, \qquad \text{curl } \mathcal{H} = -i\tilde{\omega}\tilde{\epsilon}\mathcal{E}, \tag{2}$$

and at $\omega = 2\tilde{\omega}$,

$$\text{curl } \mathbf{E} = i\omega\mu\mathbf{H}, \qquad \text{curl } \mathbf{H} = -i\omega\epsilon\mathbf{E} - i\omega\epsilon_0\mathbf{P}. \tag{3}$$

Here $\mathbf{P}$ denotes the nonlinear polarization vector, which could be expressed through the electric-field vector components at ω:

$$P^i = \chi^{ijk}\mathcal{E}_j\mathcal{E}_k, \tag{4}$$

where χ^{ijk} are the elements of the tensor of the nonlinear polarization and there is a summation over the repeating indices. Script characters and letters with tildes stand for the characteristics at the initial frequency, whereas roman or italic characters stand for the corresponding values at 2ω.

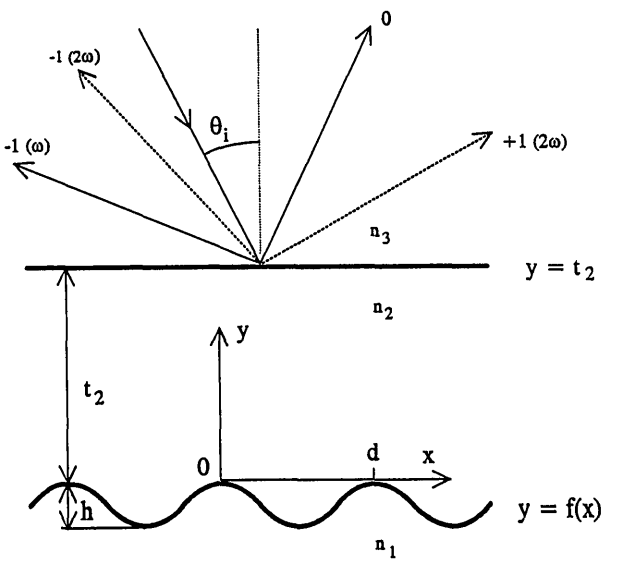

Fig. 1. Schematic representation of the corrugated waveguide under consideration.

We assume that in the Cartesian coordinate system that is initially connected with the corrugated structure χ has a diagonal (but not necessarily scalar) form, with the only nonzero components being

$$\chi^{xxx}, \chi^{yyy}, \chi^{zzz} \neq 0. \tag{5}$$

In any curvilinear coordinate system the rotational operator is defined through the Levi–Civita permutation tensor ϵ^{ijk} (Ref. 20),

$$(\text{curl } A)^i = \epsilon^{ijk} \frac{\partial A_k}{\partial x^j}, \tag{6}$$

and $\boldsymbol{\epsilon}$ and $\boldsymbol{\mu}$ are tensors that are transformed like the metric tensor $\mathbf{g}$:

$$\begin{aligned} \tilde{\mu}^{ij} &= \mu^{ij} = \mu_0 g^{ij}, \\ \tilde{\epsilon}^{ij} &= \epsilon_0 \tilde{n}^2 g^{ij}, \\ \epsilon^{ij} &= \epsilon_0 n^2 g^{ij}. \end{aligned} \tag{7}$$

Let us now introduce a specific curvilinear coordinate system, defined by

$$\begin{aligned} x^1 &= x, \\ x^2 &= y - f(x), \\ x^3 &= z. \end{aligned} \tag{8}$$

It is shown in Appendix A that Eqs. (2) and (3) take the form

$$\frac{\partial \mathcal{E}_3}{\partial x^2} = \frac{f'}{1+f'^2} \frac{\partial \mathcal{E}_3}{\partial x^1} + \frac{i}{1+f'^2} \tilde{\omega}\mu_0 \mathcal{H}_1,$$

$$\begin{aligned} \tilde{\omega}\mu_0 \frac{\partial \mathcal{H}_1}{\partial x^2} &= i\tilde{k}^2\tilde{n}^2 \mathcal{E}_3 + i \frac{\partial}{\partial x^1}\left(\frac{1}{1+f'^2} \frac{\partial \mathcal{E}_3}{\partial x^1}\right) \\ &\quad + \frac{\partial}{\partial x^1}\left(\frac{f'}{1+f'^2} \tilde{\omega}\mu_0 \mathcal{H}_1\right), \end{aligned} \tag{9a}$$

$$\begin{aligned} \frac{\partial E_3}{\partial x^2} &= \frac{f'}{1+f'^2} \frac{\partial E_3}{\partial x^1} + \frac{i}{1+f'^2} \omega\mu_0 H_1, \\ \omega\mu_0 \frac{\partial H_1}{\partial x^2} &= ik^2 n^2 E_3 + i \frac{\partial}{\partial x^1}\left(\frac{1}{1+f'^2} \frac{\partial E_3}{\partial x^1}\right) \\ &\quad + \frac{\partial}{\partial x^1}\left(\frac{f'}{1+f'^2} \omega\mu_0 H_1\right) + ik^2 \chi^z \mathcal{E}_z^2 \end{aligned} \tag{9b}$$

in TE polarization and

$$\begin{aligned} \tilde{\omega}\mu_0 \frac{\partial \mathcal{H}_3}{\partial x^2} &= -i\frac{\tilde{k}^2\tilde{n}^2}{1+f'^2} \mathcal{E}_1 + \frac{f'}{1+f'^2} \tilde{\omega}\mu_0 \frac{\partial \mathcal{H}_3}{\partial x^1}, \\ -\frac{\partial \mathcal{E}_1}{\partial x^2} &= i\tilde{\omega}\mu_0 \mathcal{H}_3 - \frac{\partial}{\partial x^1}\left(\frac{f'}{1+f'^2} \mathcal{E}_1\right) \\ &\quad + \frac{i}{\tilde{k}^2\tilde{n}^2} \frac{\partial}{\partial x^1}\left(\frac{1}{1+f'^2} \tilde{\omega}\mu_0 \frac{\partial \mathcal{H}_3}{\partial x^1}\right), \end{aligned} \tag{10a}$$

$$\begin{aligned} \omega\mu_0 \frac{\partial H_3}{\partial x^2} &= -i\frac{k^2 n^2}{1+f'^2} E_1 + \frac{f'}{1+f'^2} \omega\mu_0 \frac{\partial H_3}{\partial x^1} \\ &\quad - ik^2 \frac{1}{1+f'^2} (\chi^x \mathcal{E}_x^2 + f'\chi^y \mathcal{E}_y^2), \\ -\frac{\partial E_1}{\partial x^2} &= i\omega\mu_0 H_3 - \frac{\partial}{\partial x^1}\left(\frac{f'}{1+f'^2} E_1\right) \\ &\quad + \frac{i}{k^2 n^2} \frac{\partial}{\partial x^1}\left(\frac{1}{1+f'^2} \omega\mu_0 \frac{\partial H_3}{\partial x^1}\right) \\ &\quad - \frac{1}{n^2} \frac{\partial}{\partial x^1} \frac{f'\chi^x \mathcal{E}_x^2 - \chi^y \mathcal{E}_y^2}{1+f'^2} \end{aligned} \tag{10b}$$

in TM polarization, where we have introduced the notation $\chi^x = \chi^{xxx}$, $\chi^y = \chi^{yyy}$, $\chi^z = \chi^{zzz}$.

There are two advantages of the new coordinate system Eqs. (8). First, the equation for the corrugated boundary becomes very simple (x^2 = constant), and, second, the field components tangential to this boundary are those that directly participate in the equations: E_3, H_1 or E_1, H_3. Indeed, from the law of vector transformation, $A_i = \partial x_i / \partial x'^k A_{k'}$, we can easily obtain

$$\begin{aligned} \mathcal{H}_1 &= \mathcal{H}_x + f'(x)\mathcal{H}_y \equiv \mathbf{n} \times \boldsymbol{\mathcal{H}}, \\ \mathcal{E}_1 &= \mathcal{E}_x + f'(x)\mathcal{E}_y \equiv \mathbf{n} \times \boldsymbol{\mathcal{E}}. \end{aligned} \tag{11}$$

We can introduce a new vector $\boldsymbol{\mathcal{F}}$, defined as

$$\begin{aligned} \boldsymbol{\mathcal{F}} &= \begin{pmatrix} \mathcal{E}_3 \\ \tilde{\omega}\mu_0 \mathcal{H}_1 \end{pmatrix}, \quad \text{TE case}, \\ \boldsymbol{\mathcal{F}} &= \begin{pmatrix} \tilde{\omega}\mu_0 \mathcal{H}_3 \\ -\mathcal{E}_1 \end{pmatrix}, \quad \text{TM case}. \end{aligned} \tag{12}$$

Among the entire set of solutions we search for the one that corresponds to an incident wave with the horizontal component of the wave vector equal to $\alpha_0 = (2\pi/\lambda)\sin\theta_i$, so vector $\boldsymbol{\mathcal{F}}$ can be expanded in the form

$$\mathcal{F}(x^1, x^2) = \sum_m \exp(i\alpha_m x^1) \mathcal{F}_m(x^2), \tag{13}$$

where

$$\alpha_m = \alpha_0 + m\frac{2\pi}{d}, \qquad m = 0, \pm 1, \pm 2, \ldots, \tag{14}$$

and d stands for the period of the corrugation.

Then instead of the system of partial differential equations (9) and (10) we obtain a system of ordinary differential equations with constant coefficients, which can be written in a matrix form:

$$\frac{d\boldsymbol{\mathcal{F}}}{dx^2} = i\boldsymbol{\mathcal{T}} \mathcal{F}(x^2), \tag{15}$$

where the matrix $\boldsymbol{\mathcal{T}}$ has a block form:

$$\mathcal{T}_{mn} = \begin{bmatrix} \alpha_n \mathcal{D}_{m-n} & qC_{m-n} \\ (k^2 n^2 \delta_{mn} - \alpha_m \alpha_n C_{m-n})/q & \alpha_n \mathcal{D}_{m-n} \end{bmatrix}, \tag{16}$$

with

$$q = \begin{cases} 1 & \text{TE case} \\ k^2 n^2 & \text{TM case} \end{cases}, \tag{17}$$

and C_n and $\mathcal{D}_n$ are the Fourier components of the functions $1/(1+f'^2)$ and $f'/(1+f'^2)$, respectively.

The solution of Eq. (15) is expressed in the form:

$$\mathcal{F} = \mathcal{M}\tilde{\Phi}(x^2)\mathcal{F}_0, \tag{18}$$

where $\mathcal{M}$ is a matrix with columns equal to the eigenvectors of $\mathcal{T}$ and

$$\tilde{\Phi}_{mn} = \delta_{mn}\exp(i\rho_m x^2), \tag{19}$$

with ρ_m being the eigenvalues of $\mathcal{T}$.

If the incident wave is coming from the substrate, then the incident field and its normal derivative could be represented in the new coordinate system with the Fourier components $\mathcal{L}_m(\beta_0)$ and $\mathcal{K}_m(\beta_0)$, defined as

$$\mathcal{L}_m(\beta_n) = \frac{1}{d}\int_0^d \exp\left[i\beta_n f(x^1) - im\frac{2\pi}{d}x^1\right]dx^1,$$
$$\mathcal{K}_m(\beta_n) = \frac{1}{d}\int_0^d f'(x^1)\exp\left[i\beta_n f(x^1) - im\frac{2\pi}{d}x^1\right]dx^1, \tag{20}$$

with ${\beta_n}^2 = k^2n^2 - {\alpha_n}^2$, so that the incident field from the substrate is

$${\mathcal{F}_{1,m}}^i = \begin{bmatrix} \mathcal{L}_m(\beta_0) \\ [\beta_0\mathcal{L}_m(\beta_0) - \alpha_0\mathcal{K}_m(\beta_0)]q \end{bmatrix}. \tag{21}$$

If the incidence is from the cladding, the tangential components of the incident field are

$${\mathcal{F}_{3,m}}^i \equiv \begin{bmatrix} \mathcal{E}_z & \text{or} & \mathcal{H}_z \\ \omega\mu_0\mathcal{H}_x & \text{or} & -\mathcal{E}_x \end{bmatrix} = \begin{bmatrix} \delta_{m0} \\ \delta_{m0}\beta_0 q \end{bmatrix}. \tag{22}$$

It is necessary to separate the eigenvalues into positive (ρ^+) and negative (ρ^-) ones, depending on the sign of their imaginary part (or real part, if they are real). There are at least two reasons. First, in the upper medium the diffracted field contains only positive terms, whereas the negative terms represent the incident field; of course, in the lowest media the situation is the opposite. Second, inside the middle layer some precautions must be taken to avoid loss of precision because of the exponentially growing terms. There are several ways to do this. Probably the best is the so-called R-matrix method,[21,22] but we are using another, more direct solution: we keep in the list of unknowns not only the diffracted amplitudes in the outermost media but also the amplitudes in the middle layer. This doubles the size of the matrix but reduces the number of matrix operations and gives directly the amplitude inside the layer, which are necessary below. Of course, if the system consists of more than three media the best way is to use the R-matrix algorithm.

In each medium matrix $\mathcal{M}$ must also be ordered in the same way so that each eigenvector corresponds to its eigenvalue:

$$\mathcal{M} = \begin{bmatrix} U^+ & U^- \\ L^+ & L^- \end{bmatrix}, \tag{23}$$

where U and L denote the upper and the lower submatrices of $\mathcal{M}$.

If the upper interface is flat, then the tangential components of the field are E_z, H_x or H_z, E_x. They could easily be expressed[16] through a convolution of the components of $\mathcal{M}$ with $\mathcal{L}(-\rho_m)$:

$$\hat{U}_{mn} = \sum_p \mathcal{L}_{m-p}(-\rho_n)U_{pn},$$
$$\hat{L}_{mn} = -\sum_p \rho_n\mathcal{L}_{m-p}(-\rho_n)U_{pn}/q. \tag{24}$$

We are now ready to write the final system of equations for the unknown amplitudes inside the middle layer ($b_2^{\pm}$) and in the outermost media (${b_1}^-$ and ${b_3}^+$):

$$\begin{bmatrix} {U_1}^- & {U_2}^+ & {U_2}^-e^{(+)} & 0 \\ {L_1}^- & {L_2}^+ & {L_2}^-e^{(+)} & 0 \\ 0 & {\hat{U}_2}^+e^{(+)} & {\hat{U}_2}^- & {\hat{U}_3}^+ \\ 0 & {\hat{L}_2}^+e^{(+)} & {\hat{L}_2}^- & {\hat{L}_3}^+ \end{bmatrix}\begin{bmatrix} {b_1}^- \\ {b_2}^+ \\ {b_2}^-e^{(-)} \\ {b_3}^+ \end{bmatrix} = \begin{pmatrix} {\mathcal{F}_1}^i \\ {\mathcal{F}_3}^i \end{pmatrix}, \tag{25}$$

where the incident-field components are given by Eq. (21) or (22). Depending on the type of system (with a single or with double corrugated interfaces), either the set of U, L, or $\hat{U}$, $\hat{L}$ is used. With $e^{(+)}$, we denote a diagonal matrix with the following components:

$$e^{(\pm)}_{mn} = \delta_{mn}\exp(\pm i{\rho_m}^+ t_2), \tag{26}$$

where t_2 is the layer thickness, defined in Fig. 1.

In fact in Eq. (25) a substitution of the unknowns is made with respect to the components in the middle layer that could have growing exponential terms so that in the coefficient matrix on the left-hand side of Eq. (25) only exponentials with negative imaginary parts remain; in this way, independent of the layer thickness t_2 and the number of evanescent orders, there are no exponentially increasing terms. Moreover, for highly evanescent orders for which $\mathrm{Im}(\rho t_2)$ is very large in magnitude, the scattering on each of the interfaces becomes independent of the scattering on the other interfaces.

After Eq. (25) is solved, the components of the electric field at ω, which act as a source for the field at the frequency 2ω, are easily obtained:

$$\mathcal{E}_z \equiv \mathcal{E}_3(x^1, x^2) = \sum_{m,n}\exp(i\alpha_m x^1)U_{2,mn}\exp(i\rho_n x^2)b_{2,n} \tag{27}$$

or

$$\mathcal{E}_x(x^1, x^2) = -\frac{1}{\tilde{k}^2\tilde{n}^2}\sum_{m,n}\exp(i\alpha_m x^1)U_{2,mn}\exp(i\rho_n x^2)\rho_n b_{2,n},$$
$$\mathcal{E}_y(x^1, x^2) = \frac{1}{\tilde{k}^2\tilde{n}^2}\sum_{m,n}\exp(i\alpha_m x^1)U_{2,mn}\exp(i\rho_n x^2)$$
$$\times[\alpha_m - f'(x^1)\rho_n]b_{2,n}. \tag{28}$$

It directly follows that the source term at ω_2 has the form

$$k^2\chi^{x,y,z}{\mathcal{E}_{x,y,z}}^2(x^1, x^2) = \sum_{m,n,n'}\exp(i\xi_m x^1)\mathcal{P}_{mnn'}{}^{x,y,z}\exp[i(\rho_n + \rho_{n'})x^2], \tag{29}$$

where

$$\xi_m = 2\alpha_0 + m\frac{2\pi}{d}, \tag{30}$$

and $\mathcal{P}_{mnn'}{}^{x,y,z}$ can easily be obtained from Eq. (27) or Eqs. (28). Equation (29) implies that the source term is

periodic with respect to the x^1 axis with the grating period d, so that the solution of Eqs. (9b) or (10b) can be found in the form

$$F(x^1, x^2) = \sum_m \exp(i\xi_m x^1) F_m(x^2), \tag{31}$$

and we are able to obtain a system of ordinary differential equations similar to Eq. (15). In contrast to the case at ω_1, this system now is inhomogeneous:

$$\frac{\mathrm{d}}{\mathrm{d}x^2} F(x^2) = iTF(x^2) + iP(x^2), \tag{32}$$

where the nonhomogeneous part is equal to

$$P_m(x^2) = \sum_{nn'} P_{mnn'} \exp[i(\rho_n + \rho_{n'})x^2], \tag{33}$$

with

$$P_{mnn'} = \begin{bmatrix} 0 \\ \mathcal{P}_{mnn'}{}^z \end{bmatrix}, \qquad \text{TE case}, \tag{34a}$$

$$P_{mnn'} = \sum_p \begin{bmatrix} C_{m-p}\mathcal{P}_{pnn'}{}^x + \mathcal{D}_{m-p}\mathcal{P}_{pnn'}{}^y \\ -\dfrac{1}{k^2n^2}\,\xi_m(C_{m-p}\mathcal{P}_{pnn'}{}^y - \mathcal{D}_{m-p}\mathcal{P}_{pnn'}{}^x \end{bmatrix}, \qquad \text{TM case}. \tag{34b}$$

It is well known that the solution of Eq. (32) could be represented as a sum of the general solution $\mathbf{F}^G$ of the homogeneous equation and a particular $\mathbf{F}^P$ solution of the inhomogeneous equation. The general solution exists in the form of Eq. (18), where all the elements are calculated at ω_2. We should preserve the same notation, omitting tildes and using roman or italic instead of script letters:

$$F^G(x^2) = \mathbf{M}\Phi(x^2), \qquad \Phi_{mn} = \delta_{mn} \exp(ir_m x^2). \tag{35}$$

We should search for a particular solution, represented as a product of the general solution and a vector of unknown functions:

$$F^P(x^2) = F^G(x^2)\Psi(x^2). \tag{36}$$

Substitution of Eq. (36) into Eq. (32) leads to a set of ordinary differential equations for Ψ:

$$F^G(x^2)\Psi'(x^2) = P(x^2). \tag{37}$$

This system could be integrated directly, taking into account Eqs. (33) and (34). Then the particular solution $\mathbf{F}^P$ takes the form

$$F_m^P(x^2) = \sum_{n,n'} Q_{mnn'} \exp[i(\rho_n + \rho_{n'})x^2], \tag{38}$$

with

$$Q_{mnn'} = \sum_{p,p'} M_{mp} M_{pp'}{}^{-1} P_{p'nn'} \frac{1}{i(\rho_n + \rho_{n'} - r_p)}, \tag{39}$$

and the total solution of Eq. (32) becomes equal to

$$F_m(x^2) = \sum_n M_{mn} \exp(ir_n x^2) B_n + F_m^P(x^2). \tag{40}$$

The boundary conditions at the corrugated boundary require that the components of $\mathbf{F}$ are continuous there. The resulting algebraic system for the unknown amplitudes B_n is identical to Eq. (25). The left-hand side has exactly the same form, except that all the quantities are evaluated at ω_2. The right-hand side (source term) is changed and becomes equal to

$$\begin{pmatrix} F_m^P(0) \\ F_m^P(t_2) \end{pmatrix}. \tag{41}$$

If one of the boundaries is flat (namely, the upper), the changes introduced in matrix $\mathbf{M}$ are the same as those in matrix $\mathcal{M}$ [Eq. (24)]. The first set of components of source term (41), $\{F_m(0)\}$, is not changed. At the flat boundary the tangential components of the field are

$$E_z \equiv E_3, \qquad \omega\mu_0 H_x = i\frac{\partial E_3}{\partial x^2}, \qquad \text{TE case}, \tag{42a}$$

$$H_z \equiv H_3, \qquad -E_x = \frac{1}{k^2n^2}\left(-i\omega\mu_0 \frac{\partial H_3}{\partial x^2} + i\chi^x \mathcal{E}_x{}^2\right), \qquad \text{TM case}. \tag{42b}$$

All these vectors must be evaluated on the flat boundary $y = t_2$, which imposes the following changes in $\{F_m(t_2)\}$:

$$F_m^P(t_2) = \sum_{p,n,n'} \mathcal{L}_{m-p}(-\rho_n - \rho_{n'})\hat{Q}_{pnn'} \exp[i(\rho_n + \rho_{n'})t_2], \tag{43}$$

where matrix $\hat{\mathbf{Q}}$ is constructed from the upper part $\mathbf{Q}^U$ of matrix $\mathbf{Q}$:

$$\hat{Q}_{mnp} = \begin{bmatrix} Q_{mnp}^U \\ (\rho_n + \rho_p)Q_{mnp}^U \end{bmatrix}, \qquad \text{TE case}, \tag{44a}$$

$$\hat{Q}_{mnp} = \begin{bmatrix} Q_{mnp}^U \\ \dfrac{(\rho_n + \rho_p)}{k^2n^2} Q_{mnp}^U + \dfrac{i}{k^2n^2}\mathcal{P}_{mnp}{}^x \end{bmatrix}, \qquad \text{TM case}. \tag{44b}$$

After the unknown amplitudes of the diffracted field are obtained in the cladding and in the substrate, it is easy to evaluate the diffraction efficiencies at both ω and 2ω. If the upper interface is flat, then it is necessary just to notice that the diffracted field amplitudes $b_3{}^+$ (at ω) and $B_3{}^+$ (at 2ω) are the well-known Rayleigh coefficients in the plane-wave field expansion, so the efficiencies are equal to

$$\tilde{\eta}_{3m}(\omega) = |b_{3m}|^2 \frac{\tilde{\beta}_{3m}}{\tilde{\beta}_{j0}}\left(\frac{\tilde{q}_3}{\tilde{q}_j}\right)^{1/2},$$

$$\eta_{3m}(\omega) = |B_{3m}|^2 \frac{\beta_{3m}}{\tilde{\beta}_{j0}}\left(\frac{q_3}{\tilde{q}_j}\right)^{1/2}, \tag{45}$$

where

$$\tilde{\beta}_{pm}{}^2 = k^2\tilde{n}_p{}^2 - \alpha_m{}^2,$$

$$\beta_{pm}{}^2 = k^2 n_p{}^2 - \xi_m{}^2, \qquad p = 1, 3, \tag{46}$$

and index j in Eqs. (45) is equal to 1 or 3, depending on whether the incident wave is coming from the substrate or the cladding. The coefficient q is given by Eq. (17) and is equal to 1 for TE polarization and to $1/k^2n^2$ (or to $1/k^2\tilde{n}^2$) in the TM case.

To evaluate the diffraction efficiencies in the substrate, it is necessary to transform the field components in the substrate back into the Cartesian coordinate system. This leads us to the following expressions:

$$b_{lm}{}^{R} = \sum_{n} \hat{U}_{lmn}(\omega) b_{ln}\,,$$
$$B_{lm}{}^{R} = \sum_{n} \hat{U}_{lmn}(2\omega) B_{ln}\,, \tag{47}$$

where the matrix $\hat{\mathbf{U}}$ is determined from Eqs. (24) and the upper index R stands for the Rayleigh amplitudes. After this step Eqs. (45) can be applied with the index 3 replaced with 1.

3. RAYLEIGH–FOURIER METHOD APPLIED TO SECOND-HARMONIC GENERATION

The starting equations (3), presented in the original Cartesian coordinate system, are

$$\frac{\partial E_z}{\partial y} = i\omega\mu_0 H_x\,,$$
$$\frac{\partial E_z}{\partial x} = -i\omega\mu_0 H_y\,,$$
$$\frac{\partial H_y}{\partial x} - \frac{\partial H_x}{\partial y} = -i\omega\epsilon_0 n^2 E_z - i\omega\epsilon_0 \chi^z \mathcal{E}_z{}^2 \tag{48}$$

for TE polarization and

$$\frac{\partial H_z}{\partial y} = -i\omega\epsilon_0 n^2 E_x - i\omega\epsilon_0 \chi^x \mathcal{E}_x{}^2\,,$$
$$\frac{\partial H_z}{\partial x} = i\omega\epsilon_0 n^2 E_x + i\omega\epsilon_0 \chi^y \mathcal{E}_y{}^2\,,$$
$$\frac{\partial E_y}{\partial x} - \frac{\partial E_x}{\partial y} = -i\omega\mu_0 H_z \tag{49}$$

for TM polarization. In the linear case (at ω) Eqs. (48) and (49) have the same form without the nonlinear source term.

It is well known that, according to the Rayleigh hypothesis, the solution of these equations is represented as a sum of plane waves:

$$F(x, y) = \sum_{m} \exp(i\xi_m x + i\beta_m y) B_m{}^{R}\,, \tag{50}$$

with β given by Eqs. (46). We can use the same notation as in Section 2. The horizontal field vector components can be written as

$$\mathbf{F} \equiv \begin{Bmatrix} \begin{bmatrix} E_z \\ \omega\mu_0 H_x \end{bmatrix} \\ \begin{bmatrix} H_z \\ -E_x \end{bmatrix} \end{Bmatrix} = \xi(x)\mathbf{M}\Phi(y)\mathbf{B}_0\,, \tag{51}$$

where ξ and Φ are diagonal matrices:

$$\xi(x)_{mn} = \delta_{mn} \exp(i\xi_m x)\,,$$
$$\Phi(y)_{mn} = \delta_{mn} \exp(i\beta_m y)\,, \tag{52}$$

and the $\mathbf{M}$ matrix has a block-diagonal form, representing the fact that solutions with both positive and negative signs of β_m are possible:

$$\mathbf{M} = \begin{bmatrix} \mathbf{I} & \mathbf{I} \\ \boldsymbol{\beta} q & -\boldsymbol{\beta} q \end{bmatrix}. \tag{53}$$

In Eq. (53) $\mathbf{I}$ is the unit matrix; q is a switch, defined by Eq. (17), that depends on the polarization (17); and $\boldsymbol{\beta}$ is a diagonal matrix with elements equal to β_m.

At $y = f(x)$ the tangential components can be represented in a similar way through a matrix denoted $\hat{\mathbf{M}}$:

$$\hat{\mathbf{M}} = \begin{bmatrix} \hat{\mathbf{U}}^{+} & \hat{\mathbf{U}}^{-} \\ \hat{\mathbf{L}}^{+} & \hat{\mathbf{L}}^{-} \end{bmatrix}, \tag{54a}$$

with

$$\hat{U}_{mn}{}^{\pm} = \mathcal{L}_{m-n}(\pm\beta_n)\,,$$
$$\hat{L}_{mn}{}^{\pm} = q[\pm\beta_n \mathcal{L}_{m-n}(\pm\beta_n) - \xi_m \mathcal{K}_{m-n}(\pm\beta_n)]. \tag{54b}$$

After applying the boundary conditions at $y = f(x)$ and $y = t_2$, we can write a simple system of linear algebraic equations for the unknown field amplitudes:

$$\begin{bmatrix} \hat{U}_1{}^{-} & \hat{U}_2{}^{+} & \hat{U}_2{}^{-}e^{(+)} & 0 \\ \hat{L}_1{}^{-} & \hat{L}_2{}^{+} & \hat{L}_2{}^{-}e^{(+)} & 0 \\ 0 & U_2{}^{+}e^{(+)} & U_2{}^{-} & U_3{}^{+} \\ 0 & L_2{}^{+}e^{(+)} & L_2{}^{-} & L_3{}^{+} \end{bmatrix} \begin{bmatrix} B_1{}^{-} \\ B_2{}^{+} \\ B_2{}^{-}e^{(-)} \\ B_3{}^{+} \end{bmatrix} = \begin{bmatrix} \hat{F}_U^P \\ \hat{F}_L^P \\ F_U^P \\ F_L^P \end{bmatrix}. \tag{55}$$

If we are dealing with the linear case, then the source term simply represents the incident-wave components of Eq. (21) or (22), depending on whether the wave is incident upon the flat or the corrugated boundary. The components of the electric-field vector that act as a source for second-harmonic generation can be explicitly expressed through the amplitudes $b_m{}^{R}$ of the Rayleigh expansion inside the nonlinear layer,

$$\mathcal{E}_z = \sum_{m,\pm} \exp(i\alpha_m x)\exp(\pm i\tilde{\beta}_{2,m} y) b_{2,m}{}^{R\pm} \tag{56}$$

or

$$\mathcal{E}_x(x, y) = -\frac{1}{\tilde{k}^2\tilde{n}^2} \sum_{m,\pm} \exp(i\alpha_m x)\exp(\pm i\tilde{\beta}_{2,m} y) \times (\pm\tilde{\beta}_{2,m}) b_{2,m}{}^{R\pm}\,,$$
$$\mathcal{E}_y(x, y) = \frac{1}{\tilde{k}^2\tilde{n}^2} \sum_{m,\pm} \exp(i\alpha_m x)\exp(\pm i\tilde{\beta}_{2,m} y)\alpha_m b_{2,m}{}^{R\pm}\,, \tag{57}$$

where the summation for each α_m is carried out for the positive and the negative values of $\tilde{\beta}_m$.

After tedious but trivial calculations the particular solution at the double frequency, which acts as a source term on the right-hand side of Eq. (55), can be written in the following form, taking into account Eqs. (56) and (57):

TE case,

$$F_{m+n}^{P} \equiv \begin{bmatrix} F_U^P \\ F_L^P \end{bmatrix} = \chi^z \sum_{\pm,\pm} C_{mn}^{\pm} \begin{bmatrix} 1 \\ \tilde{\beta}_m^{\pm} + \tilde{\beta}_n^{\pm} \end{bmatrix}, \quad (58a)$$

$$\hat{F}_{m+n+p}^{P} \equiv \begin{bmatrix} \hat{F}_U^P \\ \hat{F}_L^P \end{bmatrix} = \chi^z \sum_{\pm,\pm} C_{mn}^{\pm} \begin{bmatrix} \mathcal{L}_p(\tilde{\beta}_m^{\pm} + \tilde{\beta}_n^{\pm}) \\ (\tilde{\beta}_m^{\pm} + \tilde{\beta}_n^{\pm})\mathcal{L}_p(\tilde{\beta}_m^{\pm} + \tilde{\beta}_n^{\pm}) - \xi_{m+n}\mathcal{K}_p(\tilde{\beta}_m^{\pm} + \tilde{\beta}_n^{\pm}) \end{bmatrix}; \quad (58b)$$

TM case,

$$F_{m+n}^{P} = \sum_{\pm,\pm} C_{mn}^{\pm} \begin{bmatrix} \chi^x \tilde{\beta}_m^{\pm} \tilde{\beta}_n^{\pm} (\tilde{\beta}_m^{\pm} + \tilde{\beta}_n^{\pm}) - \chi^y \alpha_m \alpha_n \xi_{m+n} \\ \chi^x \tilde{\beta}_m^{\pm} \tilde{\beta}_n^{\pm} \dfrac{\beta_{m+n}^2}{k^2 n^2} - \chi^y \alpha_m \alpha_n (\tilde{\beta}_m^{\pm} + \tilde{\beta}_n^{\pm}) \dfrac{\xi_{m+n}}{k^2 n^2} \end{bmatrix}, \quad (59a)$$

$$\hat{F}_{m+n+p}^{P} = \sum_{\pm,\pm} C_{mn}^{\pm} \left(\mathcal{L}_p(\tilde{\beta}_m^{\pm} + \tilde{\beta}_n^{\pm}) \begin{bmatrix} \chi^x \tilde{\beta}_m^{\pm} \tilde{\beta}_n^{\pm} (\tilde{\beta}_m^{\pm} + \tilde{\beta}_n^{\pm}) - \chi^y \alpha_m \alpha_n \xi_{m+n} \\ \chi^x \tilde{\beta}_m^{\pm} \tilde{\beta}_n^{\pm} \dfrac{\beta_{m+n}^2}{k^2 n^2} - \chi^y \alpha_m \alpha_n (\tilde{\beta}_m^{\pm} + \tilde{\beta}_n^{\pm}) \dfrac{\xi_{m+n}}{k^2 n^2} \end{bmatrix} \right.$$

$$\left. + \mathcal{K}_p(\tilde{\beta}_m^{\pm} + \tilde{\beta}_n^{\pm}) \begin{bmatrix} 0 \\ \chi^x \tilde{\beta}_m^{\pm} \tilde{\beta}_n^{\pm} \dfrac{\xi_{m+n}(\tilde{\beta}_m^{\pm} + \tilde{\beta}_n^{\pm})}{k^2 n^2} - \chi^y \alpha_m \alpha_n \left[1 - \dfrac{(\tilde{\beta}_m^{\pm} + \tilde{\beta}_n^{\pm})^2}{k^2 n^2} \right] \end{bmatrix} \right), \quad (59b)$$

where

$$C_{mn}^{\pm} = -\frac{k^2}{q} \frac{b_m^{\pm} b_n^{\pm} \exp[i(\tilde{\beta}_m^{\pm} + \tilde{\beta}_n^{\pm})t_2]}{(\tilde{\beta}_m^{\pm} + \tilde{\beta}_n^{\pm})^2 - \beta_{m+n}^2} \quad (60)$$

and the summation is carried out for all four combinations of positive and negative components of the field at ω_1 inside the middle layer.

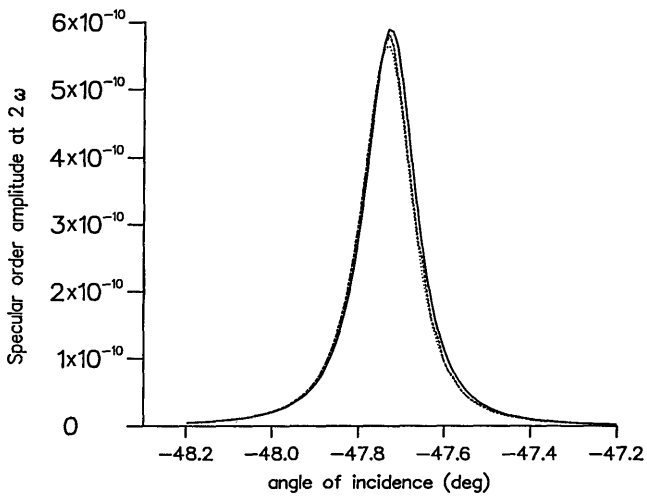

Fig. 2. Angular dependence of the modulus of the reflected zeroth-order amplitude at the second-harmonic frequency for a TM-polarized wave with wavelength 1.06 μm incident upon the flat interface, a sinusoidal corrugation at the substrate–layer interface with period of $d = 1.5$ μm and a groove depth of 0.05 μm, and refractive indices at ω for the cladding of $n_3 = 1$, the layer, $n_2 = 1.57$, and the substrate, $n_1 = 0.15 + i7.31$ and at 2ω for the cladding of $n_3 = 1$, the layer, $n_2 = 1.6 + i0.0005$, and the substrate $n_1 = 0.05 + i3.16$. The thickness of the layer is $t_2 = 0.5$ μm; $\chi^{xxx} \neq 0$, and all other components are equal to 0. Solid curve, rigorous method; dashed curve, Rayleigh method; dotted curve, classical differential theory. The solid and the dashed curves are nearly coincident.

It is possible to obtain the same expressions when the tensor of nonlinear polarization has nondiagonal terms different from zero. Let us remain with the case without polarization transfer:

$$\chi^{[x,x,z]} = \chi^{[x,y,z]} = \chi^{[y,y,z]} = 0, \quad (61)$$

where the square brackets denote all possible permutations. Then the case of TE polarization is not changed, whereas in the TM case the components of the nonlinear polarization have a more complicated form:

$$P^x = \chi^{xxx}\mathcal{E}_x^2 + (\chi^{xxy} + \chi^{xyx})\mathcal{E}_x\mathcal{E}_y + \chi^{xyy}\mathcal{E}_y^2,$$
$$P^y = \chi^{yxx}\mathcal{E}_x^2 + (\chi^{yxy} + \chi^{yyx})\mathcal{E}_x\mathcal{E}_y + \chi^{yyy}\mathcal{E}_y^2. \quad (62)$$

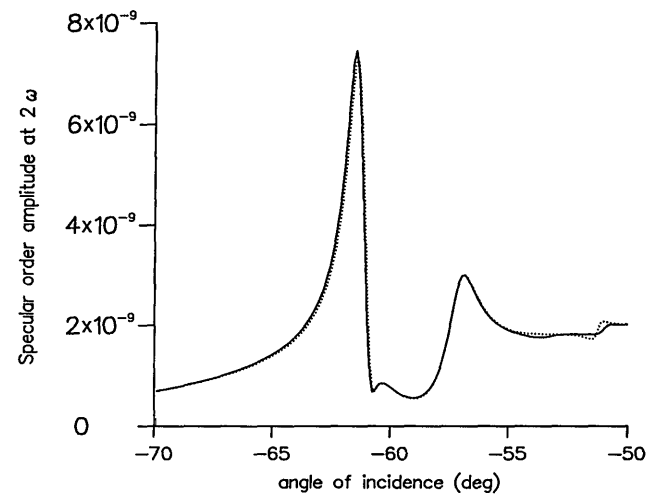

Fig. 3. Angular dependence of the modulus of the reflected zeroth-order amplitude at the second-harmonic frequency for a TE-polarized wave with wavelength 1.060 μm incident upon the corrugated interface, a sinusoidal corrugation at the cladding–layer interface with period of $d = 0.4$ μm and a groove depth of $h = 0.12$ μm, and refractive indices at ω for the cladding of $n_3 = 1$, the layer, $n_2 = 2$, and the substrate, $n_1 = 1.7$ and at 2ω for the cladding of $n_3 = 1$, the layer, $n_2 = 2.01 + i0.0005$, and the substrate, $n_1 = 1.905$. The thickness of the layer is $t_2 = 0.58$ μm. Solid curve, rigorous method; dashed curve, Rayleigh method; dotted curve, classical differential theory.

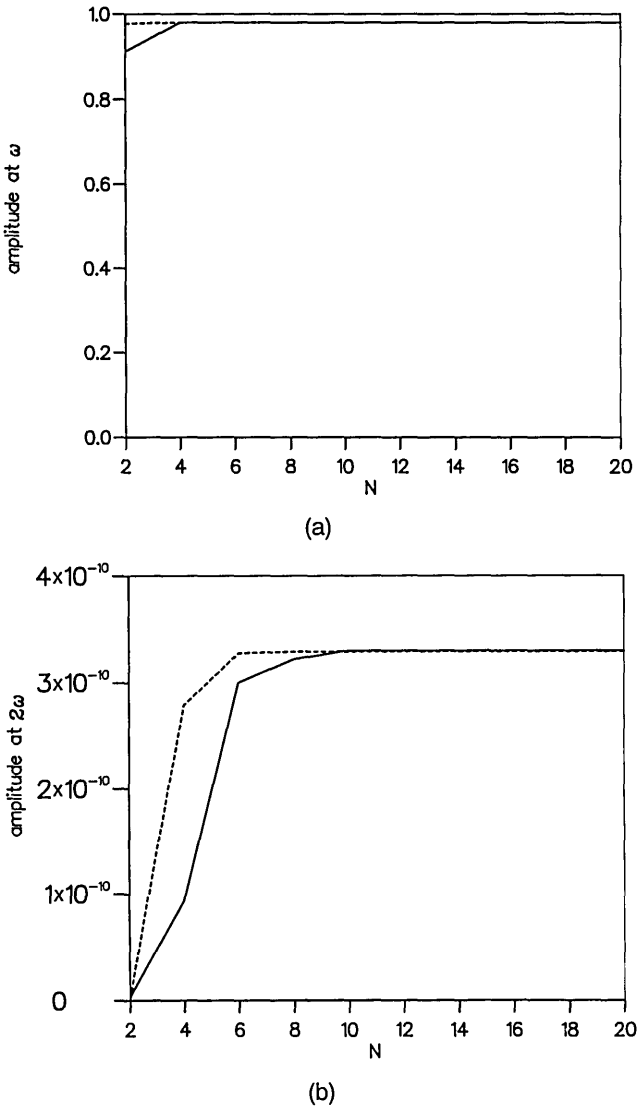

Fig. 4. Convergence of the reflected zeroth-order amplitude with respect to the truncation parameter N. All the parameters of the system and of the incident wave are the same as in Fig. 3 except for the groove depth, $h = 0.06\ \mu$m. The angle of incidence is equal to 48.05°: (a) at ω, (b) at 2ω. Solid curves, rigorous method; dashed curves, Rayleigh method.

The solution in this more general case can be obtained immediately from Eqs. (58) and (59) with the following substitutions:

$$\chi^{x}\tilde{\beta}_m^{\pm}\tilde{\beta}_n^{\pm} \rightarrow \chi^{xxx}\tilde{\beta}_m^{\pm}\tilde{\beta}_n^{\pm} - (\chi^{xxy} + \chi^{xyx})\tilde{\beta}_m^{\pm}\alpha_n + \chi^{xyy}\alpha_m\alpha_n,$$

$$\chi^{y}\alpha_m\alpha_n \rightarrow \chi^{yxx}\tilde{\beta}_m^{\pm}\tilde{\beta}_n^{\pm} - (\chi^{yxy} + \chi^{yyx})\tilde{\beta}_m^{\pm}\alpha_n + \chi^{yyy}\alpha_m\alpha_n. \quad (63)$$

The efficiencies are determined with Eqs. (45).

4. NUMERICAL RESULTS

To analyze the performance of the rigorous method as well as of the Rayleigh method, we have performed several numerical experiments. The first simulation concerns a system consisting of a metallic substrate with a corrugated surface that is covered by a layer with nonlinear properties. The upper interface is assumed to be flat. A TM-polarized wave is incident upon the flat upper interface. The only nonzero component of the tensor χ is χ^{xxx}, whose choice is determined by the method based on the classical differential formalism.[13] It must be pointed out that in the computer code based on the rigorous formalism developed in this paper there is no restriction with respect to the components of χ. Good coincidence is observed in Fig. 2 for the three methods, with the results of the new rigorous method and the Rayleigh method being indistinguishable, probably because the grating is very shallow (3.33% modulation depth h/d).

The second numerical experiment considers a grating system that consists of three dielectrics, with the middle layer having nonlinear properties. The corrugation now is put on the upper boundary, so the incident wave hits the corrugated interface, in contrast to the previous case. The polarization is TE, and the grating period is reduced significantly so that at ω there is only a single reflected order. Despite the high modulation depth (30%) there are slight differences between

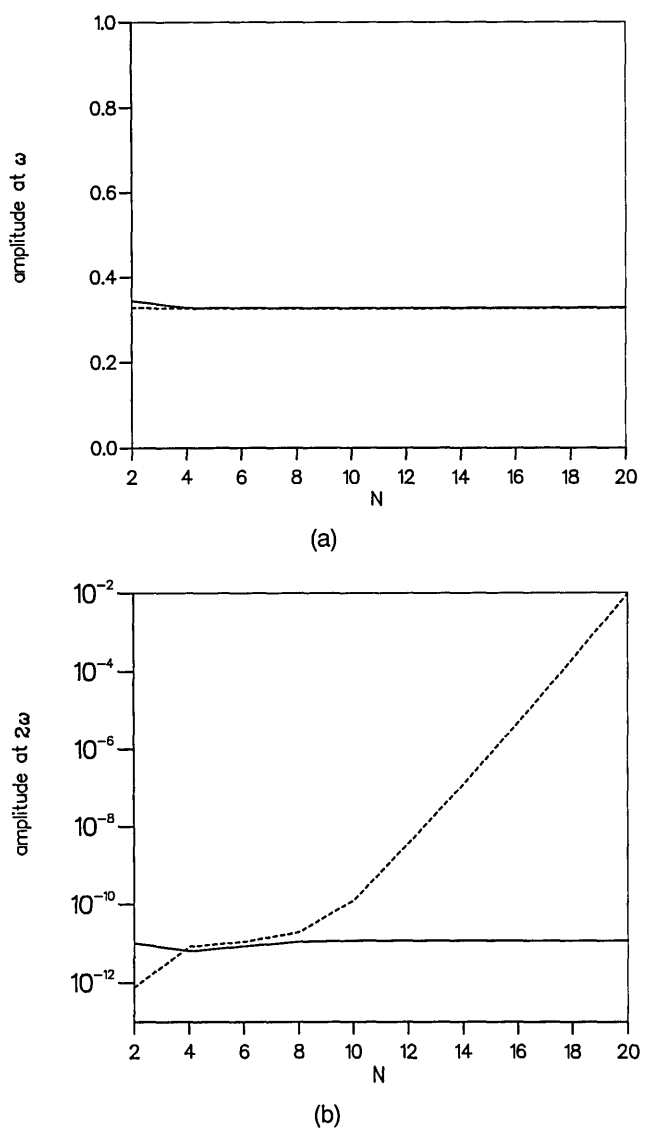

Fig. 5. Same as in Fig. 4 except for the groove depth h equal to 0.16 μm: (a) at ω, (b) at 2ω.

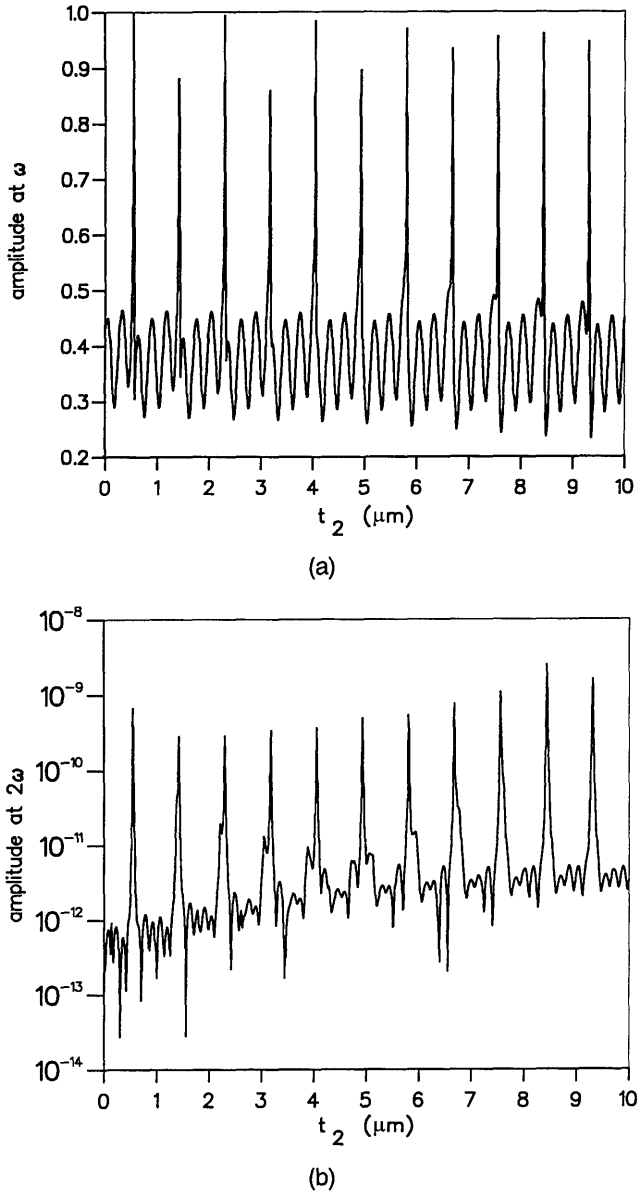

Fig. 6. Modulus of the amplitude of the reflected zeroth-order as a function of the layer thickness. All the parameters are given in Fig. 3 except the groove depth h is equal to 0.16 μm; the angle of incidence is 48.05°: rigorous method, (a) at ω, (b) at 2ω.

the three methods, as is seen in Fig. 3. It is remarkable that the Rayleigh method also gives correct results, although we are far beyond the limit of its validity ($h/d = 14\%$ for a sinusoidal grating). But the next numerical experiment shows that it could be dangerous to rely on only the results of the Rayleigh method. We have investigated the convergence of the rigorous method and of the Rayleigh method for two different modulation depth values: $h/d = 15\%$ and $h/d = 40\%$ (Figs. 4 and 5). Here the truncation parameter N represents the total number of diffraction orders taken into consideration in the calculations at 2ω; at ω they are twice as many. Whereas the rigorous method behaves well, the Rayleigh method diverges at the second-harmonic frequency, provided that the groove depth is high enough. Its convergence behavior at ω is good even for high modulation rates, a fact that was previously known, provided that the profile is sinusoidal. In contrast, at 2ω there is a divergence for deep grooves [Fig. 5(b)]. Even for a moderate value of the groove depth, corresponding to Fig. 3 (30%), if we increase N by more than 14 then the Rayleigh method diverges.

The reason for such different behavior at ω and 2ω can be understood by our taking into account the results of Van den Berg[23]: for groove-depth values greater than the limit of the validity of the Rayleigh method, the Rayleigh method can give correct results only in the far-field zone (i.e., for the amplitudes of the propagating diffracted orders at ω, in our case), whereas in the near-field zone, and, in particular, for the boundary conditions at the corrugated interface, a divergence with respect to the truncation parameter is observed. Since the near-field amplitudes of the electric field at ω are used to compute the source for the field at 2ω, the divergence of the results at 2ω comes from the fact that the source term is erroneous.

The last figure (Fig. 6) contains the dependence of the specular reflected order amplitudes at ω and at 2ω as a function of the middle (nonlinear) layer thickness. Figure 6 shows that the rigorous method is capable of dealing with thick waveguide layers without numerical instabilities. The value of 10 μm in the figure is not limited by the method; the method could deal successfully with layers several millimeters thick or more because the growing exponential terms in the scattering matrix have been removed. Note the series of resonance peaks observed both at ω and 2ω, which appear any time a higher-order mode is resonantly excited.

APPENDIX A

Starting from the definition of the matrix tensor $\mathbf{g}$ given by

$$g^{ij} = \frac{\partial x^i}{\partial x}\frac{\partial x^j}{\partial x} + \frac{\partial x^i}{\partial y}\frac{\partial x^j}{\partial y} + \frac{\partial x^i}{\partial z}\frac{\partial x^j}{\partial z}, \tag{A1}$$

it follows that, for the specific coordinate system defined by Eqs. (8), $\mathbf{g}$ takes the form

$$g^{ij} = \begin{bmatrix} 1 & -f' & 0 \\ -f' & 1+f'^2 & 0 \\ 0 & 0 & 1 \end{bmatrix}. \tag{A2}$$

In TE polarization Eq. (2) can be written as

$$\begin{aligned} \frac{\partial \mathcal{E}_3}{\partial x^1} &= -i\omega\mu_0(g^{21}\mathcal{H}_1 + g^{22}\mathcal{H}_2), \\ \frac{\partial \mathcal{E}_3}{\partial x^2} &= i\omega\mu_0(g^{11}\mathcal{H}_1 + g^{12}\mathcal{H}_2), \\ \frac{\partial \mathcal{H}_2}{\partial x^1} - \frac{\partial \mathcal{H}_1}{\partial x^2} &= -i\omega\epsilon_0\tilde{n}^2 g^{33}\mathcal{E}_3. \end{aligned} \tag{A3}$$

Substituting Eq. (A2) into Eqs. (A3) and reordering the terms leads to Eqs. (9a). Equations (9b) can be obtained in the same way.

At the second-harmonic frequency Eqs. (3) are represented in a similar form, taking into account the covariant representation, Eq. (4), of the nonlinear polarization

vector **P** and the transformation law for the third-order rank tensor χ:

$$\chi^{i'j'k'} = \sum_{ijk}^{3} \frac{\partial x^{i'}}{\partial x^{i}} \frac{\partial x^{j'}}{\partial x^{j}} \frac{\partial x^{k'}}{\partial x^{k}} \chi^{ijk}. \tag{A4}$$

*On leave from the Institute of Solid State Physics, Bulgarian Academy of Sciences, 72, Tzarigradsko Chaussee Boulevard, 1784 Sofia, Bulgaria.

REFERENCES

1. J. E. Sipe and G. I. Stegeman, "Nonlinear optical response of metal surfaces," in *Surface Polaritons, Electromagnetic Waves at Surfaces and Interfaces*, V. M. Agranovich and D. L. Mills, eds. (North-Holland, Amsterdam, 1982), pp. 661–701 and references therein.
2. R. Reinisch and M. Nevière, "Gratings as electromagnetic field amplifiers for second-harmonic generation," in *Scattering in Volumes and Surfaces*, M. Nieto-Vesperinas and J. C. Dainty, eds. (North-Holland, Amsterdam, 1990), pp. 269–285, and references therein.
3. R. Reinisch, G. Vitrant, and M. Nevière, "Electromagnetic resonance induced nonlinear phenomena," in *Nonlinear Waves in Solid State Physics*, A. D. Boardman, M. Betolotty, and T. Twardowsky, eds. (Plenum, New York, 1990), pp. 435–461, and references therein.
4. V. M. Agranovich and D. L. Mills, eds., *Surface Polaritons, Electromagnetic Waves at Surfaces and Interfaces* (North-Holland, Amsterdam, 1982).
5. T. Suzuki and T. F. Heinz, "Second-harmonic diffraction from a monolayer gratin," Opt. Lett. **14,** 1201–1203 (1989).
6. H. J. Simon, C. Huang, J. C. Quail, and Z. Chen, "Second-harmonic generation with surface plasmons from a silvered quartz grating," Phys. Rev. B **38,** 7408–7414 (1988).
7. Z. Chen and H. J. Simon, "Optical second-harmonic generation with coupled surface plasmons from a multilayer silver-quartz grating," Opt. Lett. **13,** 1008–1010 (1988).
8. H. J. Simon and Z. Chen, "Optical second-harmonic generation with grating-coupled surface plasmons from a quartz-silver-quartz grating structure," Phys. Rev. B **39,** 3077–3085 (1989).
9. R. Reinisch and M. Nevière, "Electromagnetic theory of diffraction in nonlinear optics and surface enhanced nonlinear optical effects," Phys. Rev. **28,** 1870–1885 (1983).
10. M. Nevière, P. Vincent, D. Maystre, R. Reinisch, and J. L. Coutaz, "Differential theory for metallic gratings in nonlinear optics: second-harmonic generation," J. Opt. Soc. Am. B **5,** 330–337 (1988).
11. D. Maystre, M. Nevière, R. Reinisch, and J. L. Coutaz, "Integral theory for metallic gratings in nonlinear optics and comparison with experimental results on second-harmonic generation," J. Opt. Soc. Am. B **5,** 338–346 (1988).
12. D. Maystre, M. Nevière, and R. Reinisch, "Nonlinear polarization inside metals: a mathematical study of the free electron model," Appl. Phys. A **39,** 115–121 (1986).
13. H. Akhouayri, M. Nevière, P. Vincent, and R. Reinisch, "Second harmonic generation in a corrugated waveguide," Mol. Cryst. Liq. Cryst. Sci. Technol. Sec. B (to be published).
14. J. Chandezon, D. Maystre, and G. Raoult, "A new theoretical method for diffraction gratings and its numerical application," J. Opt. (Paris) **11,** 235–241 (1980).
15. J. Chandezon, M. T. Dupuis, G. Cornet, and D. Maystre, "Multicoated gratings: a differential formalism applicable in the entire optical region," J. Opt. Soc. Am. **72,** 839–847 (1982).
16. E. Popov and L. Mashev, "Rigorous electromagnetic treatment of planar corrugated waveguides," J. Opt. Commun. **7,** 127–131 (1986).
17. E. Popov and L. Mashev, "Convergence of Rayleigh–Fourier method and rigorous differential method for relief diffraction gratings," Opt. Acta **33,** 593–605 (1986).
18. E. Popov and L. Mashev, "Convergence of Rayleigh–Fourier method and rigorous differential method for relief diffraction gratings—non-sinusoidal profile," Opt. Acta **34,** 155–158 (1987).
19. M. Cadilhac, "Some mathematical aspects of the grating theory," in *Electromagnetic Theory of Gratings*, R. Petit, ed. (Springer-Verlag, Berlin, 1980), pp. 52–62, and references cited therein.
20. B. Spain, *Tensor Calculus* (Oliver and Boyd, Edinburgh, and Interscience, New York, 1953), p. 60.
21. D. J. Zvijac and J. C. Light, "*R*-matrix theory for collinear chemical reactions," Chem. Phys. **12,** 237–251 (1976).
22. J. C. Light and R. B. Walker, "An *R*-matrix approach to the solution of coupled equations for atom–molecule reactive scattering," J. Chem. Phys. **65,** 4272–4282 (1976).
23. P. M. Van den Berg, "Reflection by a grating: Rayleigh methods," J. Opt. Soc. Am. **71,** 1224–1229 (1981).